JOURNAL OF AGRICULTURAL AND FOOD CHEMISTRY

Induction of Apoptosis by Vitamin D_2, Ergocalciferol, via Reactive Oxygen Species Generation, Glutathione Depletion, and Caspase Activation in Human Leukemia Cells

WEI-JEN CHEN,[†] YU-TING HUANG,[‡] MEI-LI WU,[§] TZOU-CHI HUANG,[§] CHI-TANG HO,[⊥,▽] AND MIN-HSIUNG PAN*,[‡]

Department of Biomedical Sciences, Chung Shan Medical University, No. 110, Section 1, Chien-Kuo N. Road, Taichung 402, Taiwan; Department of Seafood Science, National Kaohsiung Marine University, No. 142, Hai-Chuan Road, Nan-Tzu, Kaohsiung 811, Taiwan; Department of Food Science, National Pingtung University, 912 Pingtung, Taiwan; Department of Food Science, Rutgers University, New Brunswick, New Jersey 08901-8520; and Graduate Institute of Food Science and Technology, National Taiwan University, Taipei, Taiwan

This study demonstrated that ergocalciferol was able to inhibit leukemia cell growth in a concentration-dependent manner. Exploration of the acting mechanisms involved this event revealed that ergocalciferol induced DNA fragmentation and increased sub-G1 DNA contents in HL-60 cells, both of which are hallmarks of apoptosis. Analysis of the integrity of mitochondria demonstrated that ergocalciferol caused loss of mitochondrial membrane potential with release cytochrome *c* to cytosol, generation of reactive oxygen species (ROS), and depletion of glutathione (GSH), suggesting that ergocalciferol may induce apoptosis in HL-60 cells through a ROS-dependent pathway. Further results show that caspases-2, -3, -6, and -9 were all activated by ergocalciferol, together with cleavage of the downstream caspase-3 targets, DNA fragmentation factor (DFF-45), and poly(ADP-ribose) polymerase. In addition, ergocalciferol led to the increase in pro-apoptotic factor Bax accompanied with the decrease in anti-apoptotic member Mcl-1, and the reduced Mcl-1 to Bax ratio may be a critical event concerning mitochondrial decay by ergocalciferol. Furthermore, ergocalciferol also led to induction of Fas death receptor closely linked to caspase-2 activation, suggesting the involvement of a Fas-mediated pathway in ergocalciferol-induced apoptosis. Totally, these findings suggest that ergocalciferol causes HL-60 apoptosis via a modulation of mitochondria involving ROS production, GSH depletion, caspase activation, and Fas induction. On the basis of anticancer activity of ergocalciferol, it may be feasible to develop chemopreventive agents from edible mushrooms or hop.

KEYWORDS: Ergocalciferol; apoptosis; mushrooms; reactive oxygen species (ROS); mitochondria; cytochrome *c*; caspase; Bax; Mcl-1; Fas

INTRODUCTION

Mushrooms have been part of plant-based diets and consumed since ancient times because of their desirable taste and nutritional values. It is known that over thousands of mushroom species exist, but only <10% species are edible. Recently, cancer researchers have paid more attention to mushrooms because some biologically active compounds in mushrooms may possess anticancer properties. Of bioactive constituents in mushrooms, vitamin D compounds have been recognized to play a vital role in the prevention of cancer cell development and proliferation (*1, 2*). Provitamin D_2 and vitamin D_2 have also been identified recently in hop plant (*Humulus lupulus* L.) (*3*).

The natural vitamin D can be divided into animal-based vitamin D_3 and plant-based vitamin D_2. Vitamin D_3 (also known as cholecalciferol) controls calcium homeostasis and bone metabolism and has been considered to be a cancer-preventive agent due to its regulatory effects on proliferation, differentiation, and apoptosis in cancer cells (*4–6*). In mammals, vitamin D_3 can be synthesized in the skin under sunlight exposure or derived from dietary sources. Then, vitamin D_3 is metabolized in the liver and kidney and finally converted to its active form, 1α,25-dihydroxyvitamin D_3 [1α,25$(OH)_2D_3$; calcitriol]. 1α,25-

* Author to whom correspondence should be addressed (telephone 886-7-361-7141, ext. 3623; fax 886-7-361-1261; e-mail mhpan@mail.nkmu.edu.tw).
[†] Chung Shan Medical University.
[‡] National Kaohsiung Marine University.
[§] National Pingtung University.
[⊥] Rutgers University.
[▽] National Taiwan University.

10.1021/jf0730744 CCC: $40.75
Published on Web 04/03/2008

$(OH)_2D_3$ induces the differentiation of myeloid leukemia (*7, 8*) and inhibits the proliferation of various types of malignant cells, including breast (*9*), prostate (*10*), colon (*11*), and squamous cancer cells (*12*).

Similar to vitamin D_3 in animals, vitamin D_2 (ergocalciferol) occurs in plants and is a natural vitamin D_3 analogue. It is generated from provitamin D_2 (ergosterol) by the exposure of sunshine and has an extra methyl group at C_{24} and a double bond between C_{22} and C_{23} as compared with vitamin D_3. Vitamins D_2 and D_3 are assumed to have an equal potency for mammals and share the same metabolic route, that is, 25-hydroxylation in the liver and then 1α-hydroxylation in the kidney (*5*). 25-Hydroxylated metabolites of vitamin D_2 equal to those of vitamin D_3involving the circulatory form of vitamin D_2, 25-dihydroxyvitamin D_2 ($25OHD_2$), and the active form of vitamin D_2, 1α,25-dihydroxyvitamin D_2 [$1\alpha,25(OH)_2D_2$)], are identified in human sera (*13*). It is noted that the metabolic routes of vitamin D_2 are not completely the same as those of vitamin D_3. In addition to 25-hydroxylation, 24-hydroxylation of vitamin D_2, an alternative and particular metabolic route for vitamin D_2, has been found in an early animal study (*14*), and a further study by Mawer et al. (*15*) has demonstrated that several 24-hydroxylation-based vitamin D_2 metabolites such as 24-hydroxyvitamin D_2 ($24OHD_2$) and 1α,24-dihydroxyvitamin D_2 [$1\alpha,24(OH)_2D_2$] can be detectable in human sera and naturally occurred by administration with large doses of vitamin D_2 or parathyroid hormone infusion. Significantly, $1\alpha,24(OH)_2D_2$ has a potent antiproliferative activity with a low calcemic effect relative to $1\alpha,25(OH)_2D_3$ (*16, 17*), suggesting that vitamin D_2-rich foods such as edible mushrooms may play a vital role in cancer prevention. In addition, many studies have confirmed that vitamin D_2 analogues have anticancer activity (*18–20*). However, this is the first study to discuss the apoptotic mechanisms of vitamin D2 in detail.

Apoptosis, a defined type of cell death, involves a sophisticated network of tightly ordered molecular events that are highly conserved from lower eukaryotes to mammals. Two well-established mechanisms involving apoptotic cell death have been characterized. One is mediated by death receptors, which interact with their ligands including Fas, tumor necrosis factor receptor (TNFR), death receptor 3 (DR3), DR4, and DR5 (*21*). The other is involved in the participation of mitochondria, for most forms of apoptosis in response to cellular stress, loss of survival factors, and developmental cues (*22*). Recent studies of the endoplasmic reticulum (ER) as a third subcellular compartment containing caspase-12 were implicated in apoptotic execution induced by ER stress (*23–25*). Induction of apoptosis by natural phytochemicals in malignant cells may offer a promising tactic for cancer chemoprevention (*26, 27*).

A recent epidemiological study indicates that mushroom intake has a protective effect on the risk of gastric cancer (*28*). However, the constituents in mushrooms contributing to antitumor activity have not been fully understood. In this study, we presumed that vitamin D_2 may be one of the active antitumor agents in mushrooms besides β-glucan and phellinone. To this end, we determined and compared the cytotoxic effects of provitamin D_2 (ergosterol) and vitamin D_2 (ergocalciferol) in the human leukemia HL-60 cell line. We found that both provitamin D_2 (ergosterol) and vitamin D_2 (ergocalciferol) induced apoptosis in HL-60 cells and that vitamin D_2 had a more profound effect. Further exploration of the action mechanism of apoptosis induced by vitamin D_2 demonstrated that ROS production, GSH depletion, and caspase cascades were involved in the apoptotic machinery. These findings may provide a molecular basis for cancer-preventive activity of edible mushrooms.

MATERIALS AND METHODS

Materials. Ergosterol and (95%) and ergocalciferol (98%) were purchased from Sigma Chemical Co. (St. Louis, MO), and their purities were 95 and 98%, respectively. Propidium iodide (PI) and horseradish peroxidase-conjugated anti-mouse and anti-rabbit IgG were available from Sigma Chemical Co.

Cell Culture and Cell Extract Preparation. Human promyelocytic leukemia (HL-60) cells obtained from American Type Culture Collection (Rockville, MD) were grown in RPMI-1640, supplemented with 15% fetal calf serum (Gibco BRL, Grand Island, NY), 100 units/mL penicillin, 100 μg/mL streptomycin, and 2 mM L-glutamine (Life Technologies, Inc., Grand Island, NY) and kept at 37 °C in a humidified atmosphere of 5% CO_2 in air. At the end of incubation, cells were harvested, washed with cold phosphate-buffered saline twice, and homogenized in a Gold lysis buffer [50 mM Tris-HCl, pH 8.0, 5 mM EDTA, 150 mM NaCl, 0.5% (v/v) Nonidet P-40, 0.5 mM phenylmethyanesulfonyl fluoride, and 0.5 mM dithiothreitol] for 30 min at 4 °C. Afterward, the lysates were centrifuged at 12000*g* for 30 min, and then the supernatants were collected as whole cell extracts. Protein determination was performed according to the method of Bradford (kit available from Bio-Rad, Richmond, CA) with BSA as standard.

Determination of Cell Viability. Cell viability was assayed with 3-(4,5-dimethylthiazol-2-yl)-2,5-diphenyl tetrazolium bromide (MTT). Briefly, HL-60 cells were plated at a density of 1×10^5 cells/mL into 24-well plates. After overnight growth, cells were treated with a series of concentrations of ergosterol or ergocalciferol for 24 h. The final concentration of dimethyl sulfoxide in the culture medium was <0.1%. At the end of treatment, 30 μL of MTT was added, and cells were incubated for an additional 4 h. Cell viability was determined by scanning with an enzyme-linked immunosorbent assay reader with a 570 nm filter.

DNA Extraction and Electrophoresis Analysis. HL-60 cells (2×10^5 cells/mL) were harvested, washed with PBS, and then lysed with digestion buffer containing 0.5% sarkosyl, 0.5 mg/mL proteinase K, 50 mM tris(hydroxymethyl)aminomethane (pH 8.0), and 10 mM EDTA at 56 °C for 3 h and treated with RNase A (0.5 μg/mL) for another 2 h at 56 °C. DNA was extracted by phenol/chloroform/isoamyl alcohol (25:24:1) before loading and analyzed by 2% agarose gel electrophoresis. The agarose gels were run at 50 V for 120 min in TBE buffer (Tris-borate/EDTA electrophoresis buffer). Approximately 20 μg of DNA was loaded in each well, subjected to electrophoresis, visualized under UV light, and then photographed.

Flow Cytometric Cell Analysis. HL-60 cells (2×10^5) were cultured in 60 mm Petri dishes and incubated for various times. The cells were then harvested, washed with PBS, resuspended in 200 μL of PBS, and fixed in 800 μL of iced 100% ethanol at −20 °C. They were left to stand overnight, and then the cell pellets were collected by centrifugation, resuspended in 1 mL of hypotonic buffer (0.5% Triton X-100 in PBS and 0.5 μg/mL RNase A), and incubated at 37 °C for 30 min. Next, 1 mL of propidium iodide solution (50 μg/mL) was added, and the mixture was allowed to stand on ice for 30 min. Fluorescence emitted from the propidium iodide−DNA complex was quantified after excitation of the fluorescent dye by FACScan cytometry (Becton Dickenson, San Jose, CA).

Annexin V-FITC Binding Assay. The cells were grown and treated with 60 μM ergocalciferol for 15 min, harvested, and then washed twice with cold PBS. The washed cells were equilibrated for 10 min in binding buffer (10 mM HEPES, 140 mM NaCl, 2.5 mM $CaCl_2$, pH 7.4). After equilibration, the binding buffer was removed, and fresh binding buffer but containing annexin V-Alexa Fluor 488 conjugates (Molecular Probes) and propidium iodide were added for 15 min of incubation. Apoptotic cells were detected by FACScan cytometry (Becton Dickenson).

Determination of ROS Generation and Glutathione (GSH) Variation. ROS production was monitored by flow cytometry using dichlorodihydrofluorescein diacetate (DCHF-DA) and dihydroethidium

(DHE). This dye is a stable, nonpolar compound that readily diffuses into cells and is hydrolyzed by intracellular esterase to yield the DCHF, trapped within the cells. Hydrogen peroxide (H_2O_2) or low molecular weight peroxides produced by the cells oxidize DCHF to the highly fluorescent compound 2′,7′-dichlorofluorescein (DCF). Thus, the fluorescence intensity is proportional to the amount of hydrogen peroxide produced by the cells. Dihydroethidium (DHE) was used as a probe, recognizing mainly the oxygen species superoxide anion. The thioreactive fluorescent dye 5-chloromethylfluorescein diacetate (CMFDA) was assayed for GSH determination. CFMDA forms a GSH adduct in a reaction catalyzed by glutathione-*S*-transferase. After conjugation with GSH, CMFDA is hydrolyzed to the fluorescent 5-chloromethylfluorescein by cellular esterase (*29*). Cells were pretreated with ergocalciferol (60 μM) for 60 or 30 min and then incubated with DCHF-DA (20 μM), DHE (20 μM), or CFMDA (30 μM) for a further 30 min at 37 °C. The fluorescent intensity was monitored by FACScan cytometry. Histograms were analyzed using Cell Quest software and were compared with histograms of untreated control cells.

Determination of Mitochondrial Membrane Potential ($\Delta\Psi$m). The change of the mitochondrial transmembrane potential is monitored by flow cytometry. Briefly, HL-60 cells were cultured and allowed to reach exponential growth for 24 h before treatment. The cells were harvested for 30 min after treatment with 60 μM ergocalciferol. Changes in $\Delta\Psi$m were determined by uptake of the 40 nM 3,3′-dihexyloxacarbocyanine [DiOC6(3)] (Molecular Probes, Eugene, OR) into mitochondria. Fluorescence was measured using a FACScan (Becton Dickinson) after staining of the cells for 30 min at 37 °C. Histograms are analyzed using Cell Quest software and are compared with histograms of control untreated cells. Untreated control cells were used to determine the normal uptake of this cation, and the percentage of treated cells with a low MMP was then calculated.

Subcellular Fractionations and Determination of Cytochrome *c* Release. Mitochondrial and cytosolic (S100) fractions were prepared as described previously (*30–33*). Briefly, after 60 μM ergocalciferol treatment, cells were washed twice in ice-cold PBS and then resuspended in homogenizing buffer [250 mM sucrose, 20 mM HEPES, 10 mM KCl, 1.5 mM $MgCl_2$, 1 mM EDTA, 1 mM EGTA, 1 mM dithiolthione, 17 μg/mL phenylmetanesulfonyl fluoride, 8 μg/mL aprotinin, 2 μg/mL leupeptin (pH 7.4)]. After 30 min of incubation on ice, cells were passed through a needle 10 times. Unbroken cells and nuclei were pelleted by centrifugation at 750*g* for 10 min. The supernatant was spun at 10000*g* for 15 min to pellet the mitochondrial fraction, which was resuspended in homogenizing buffer. The remaining supernatant was spun at 100000*g* for 1 h, and the resultant supernatant was designated the cytosolic (S100) fraction. The determination of cytochrome*c* release was performed by Western blotting as follows.

Western Blot Analysis. Equal amounts of total cellular proteins (50 μg) were resolved by SDS−polyacrylamide gel electrophoresis (SDS-PAGE), transferred onto polyvinylidene difluoride (PVDF) membranes (Immobilon P, Millipore, Bedford, MA) with transfer buffer composed of 25 mM Tris-HCl (pH 8.9), 192 mM glycine, and 20% methanol, and then probed with primary antibody followed by secondary antibody conjugated with horseradish peroxidase. The immunocomplexes were visualized with enhanced chemiluminescence kits (Amersham, U.K.), and the intensity of the band was scanned and quantified by densitometer. The primary antibodies used include anticaspased-3 and -9 (PharMingen, San Diego, CA), anti-Bcl-2, anti-Bcl-X_L, anti-Bad, anti-Bax (Santa Cruz Biotechnology, Santa Cruz, CA), antipoly(ADP-ribose) polymerase (PARP) (UBI Inc., Lake Placid, NY), anti-Bag-1, anti-Mcl-1 (R and D System Inc., Minneapolis, MN), anti-β-Actin (Transduction Laboratory, Lexington, KY), and anti-DFF45/inhibitor of caspase activated DNase (ICAD) (MBL, Naka-Ku, Nagoya, Japan) antibodies.

Assay of Caspase Activity. HL-60 cells were treated with 60 μM ergocalciferol for indicated times and then collected and washed with PBS and suspended in 25 mM HEPES (pH 7.5) containing 5 mM $MgCl_2$, 5 mM EDTA, 5 mM dithiothione, 2 mM phenylmethanesulfonyl fluoride, 10 μg/mL pepstatin A, and 10 μg/mL leupeptin. Cell lysates were clarified by centrifugation at 12000*g* for 20 min at 4 °C. The caspase activity in the supernatant was determined by a fluorogenic assay (Promega CaspACE Assay System Corp., Madison, WI). Briefly, 100 μg of total protein was incubated with a 50 μM concentration of substrate Ac-Try-Val-Ala-Asp-AMC (Ac-YVAD) (caspase-1-specific substrate), Ac-Val-Asp-Val-Ala-Asp-AMC (Ac-VDVAD-AMC) (caspase-2-specific substrate), Ac-Asp-Glu-Val-Asp-AMC (Ac-DEVD-AMC) (caspase-3-specific substrate), Ac-Ile-Glu-Thr-Asp-AMC (Ac-IETD-AMC) (caspase-8-specific substrate), or Ac-Leu-Glu-His-Asp-AMC (Ac-LEHD-AMC) (caspase-9-specific substrate) at 30 °C for 1 h. The release of methylcoumaryl-7-amine (AMC) was measured by excitation at 360 and emission at 460 nm using a fluorescence spectrophotometer (Hitachi F-4500).

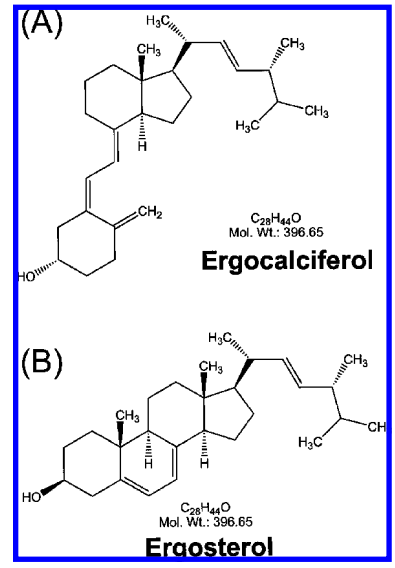

Figure 1. Chemical structures of (**A**) ergocalciferol and (**B**) ergosterol.

Statistical Analysis. Data are presented as means ± standard error (SE) for the indicated number of independently performed experiments. Mean values between the groups were compared using Student's unpaired two-tailed *t* test. All statistical tests were two-sided, and differences were considered to be significant when $p < 0.05$.

RESULTS

Both Ergosterol and Ergocalciferol Caused Dose-Dependent Reduction in Leukemia Cell Viability. We evaluated the growth-inhibitory potential of ergosterol and ergocalciferol on human leukemia HL-60 cell line. Various doses of ergosterol or ergocalciferol were added to exponential HL-60 cells for 24 h of incubation, and the curve of cell growth was determined by means of the MTT method. As shown in **Figures 1** and **2A**, both ergosterol and ergocalciferol exhibit the cytotoxic effects on HL-60 cell growth in a concentration-dependent manner, and ergocalciferol is more effective than ergosterol as a chemopreventive agent against leukemia cells within the range of low concentration. The data imply that ergosterol and ergocalciferol might suppress cancer cell proliferation or induce cancer cells undergoing apoptosis that lead to cell growth inhibition.

Ergocalciferol Promoted HL-60 Cells Undergoing Apoptosis. Because HL-60 cells were more sensitive to ergocalciferol than ergosterol, we further focused on ergocalciferol to study the mechanisms by which ergocalciferol suppresses cell viability. To determine whether the inhibition of cell growth by ergocalciferol results from the induction of apoptosis, DNA fragmentation, a hallmark of apoptosis, was demonstrated by incubating HL-60 cells with 100 μM ergosterol and ergocalciferol, respectively. DNA fragmentation was found in ergocalciferol-treated cells but not found in ergosterol. HL-60 cells were further treated with different doses of ergocalciferol for 24 h. DNA fragmentation became apparent at 60 μM ergocalciferol treatment, and these DNA fragmentation responses were

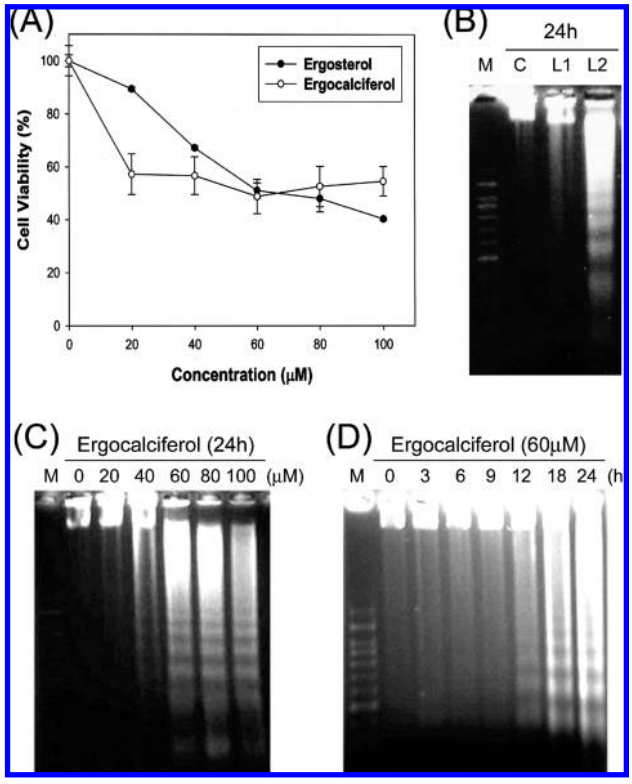

Figure 2. Effects of ergocalciferol and ergosterol on cell viability and DNA fragmentation. (**A**) HL-60 cells were treated with various concentrations of ergocalciferol or ergosterol for 24 h. Cell viability was then determined by the MTT assay as described under Materials and Methods. Each experiment was independently performed three times and expressed as mean ± SE. (**B**) Cells were treated with 100 μM ergosterol (L1) and ergocalciferol (L2) for 24 h. (**C**) HL-60 cells were treated with increasing doses of ergocalciferol for 24 h or (**D**) with 60 μM ergocalciferol for the indicated time, and internucleosomal DNA fragmentation was analyzed by agarose gel electrophoresis. M, one hundred base pair DNA ladder size marker.

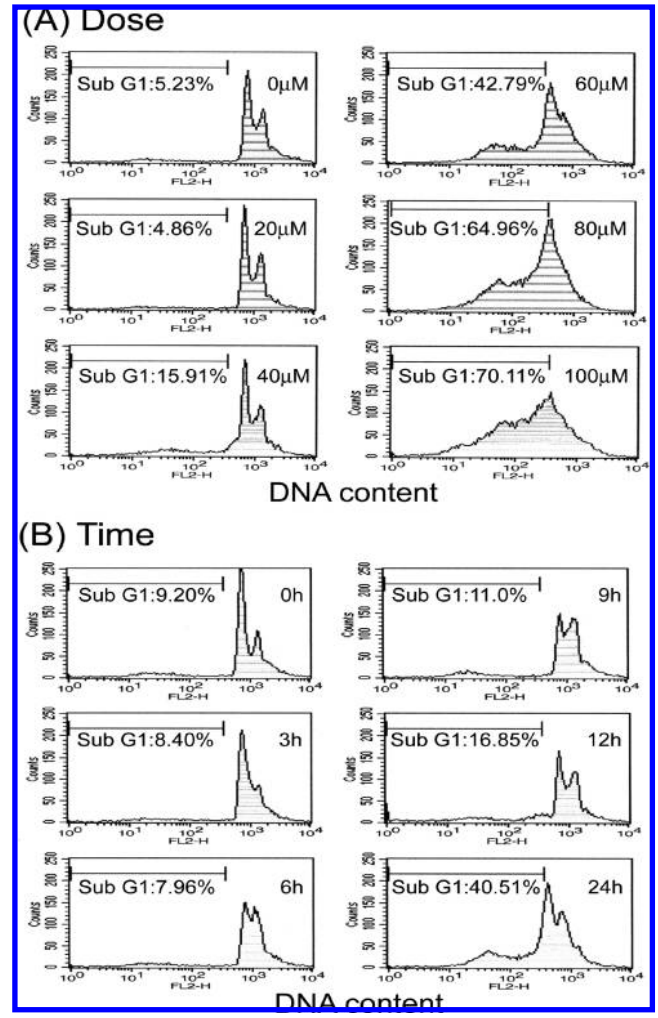

Figure 3. Determination of sub-G1 cells in ergocalciferol-treated HL-60 cells. (**A**) HL-60 cells were treated with various concentrations of ergocalciferol as indicated for 24 h. (**B**) HL-60 cells were treated with 60 μM ergocalciferol for the indicated times, and then the ratio of sub-G1 cells was analyzed by flow cytometry. Sub-G1 population represents apoptotic cells with a lower DNA content.

dose-dependent (**Figure 2C**). When cells were treated with 60 μM ergocalciferol, DNA ladders were just visible as early as 12 h after treatment and gradually increased from 6 to 24 h (**Figure 2D**).

To investigate the effect of ergocalciferol on cell cycle progression, the DNA content of HL-60 cells treated with ergocalciferol at various concentrations and for various time periods was analyzed by flow cytometry. A sub-G1 DNA peak, which has been suggested to be the apoptotic DNA (*34, 35*), was detected in ergocalciferol-treated cells, and the percentages of apoptotic HL-60 cells (sub-G1 population) were gradually increased by 5.23, 4.86, 15.91, 42.79, 64.96, and 70.11% for 0, 20, 40, 60, 80, and 100 μM treatments, respectively (**Figure 3A**). Time-corresponding increases in sub-G1 population of HL-60 cells were also found for the indicated times with 60 μM ergocalciferol treatment (**Figure 3B**). Interestingly, the increased levels of DNA fragment and sub-G1 population are similar and the time the DNA ladder occurred is also paralleled to sub-G1 peak appearance, suggesting that ergocalciferol induces HL-60 leukemia cell apoptosis.

To further elucidate that ergocalciferol triggers apoptosis rather than necrosis, the early apoptotic morphological change in membrane integrity such as phosphatidylserine (PS) translocation was monitored by annexin V staining. Fluorescence intensity clearly displays a significant increase from 173.38 to 418.98 during ergocalciferol treatment in HL-60 cells (**Figure 4A**), providing the extra evidence to prove that ergocalciferol will cause apoptosis.

Involvement of GSH Depletion and ROS Production in Ergocalciferol-Induced Apoptosis. Glutathione (GSH) has been considered to be an important antioxidant to protect cell against apoptosis by removing toxic hydrogen peroxide from cells in a reaction catalyzed by glutathione peroxidase (*36, 37*), and the depletion of GSH within cells appears to be a reason for intracellular ROS accumulation. Using the fluorescent probe CMFDA to determine the amount of GSH within cells, we found that ergocalciferol treatment led to CMFDA fluorescence intensity shifted to the left from 110.13 to 58.48 at 30 min, reflecting that ergocalciferol reduces the intracellular GSH levels (**Figure 4B**).

ROS such as superoxide and hydrogen peroxide have been indicated to play an important role in the induction of apoptosis (*38, 39*). To assess whether the reduction of GSH by ergocalciferol would result in ROS generation, the levels of superoxide and hydrogen peroxide were determined by flow cytometry using fluorescent probes DHE (specific for superoxide) and DCHF-DA (specific for hydrogen peroxide). After 30 min of incubation with ergocalciferol, the increased levels of

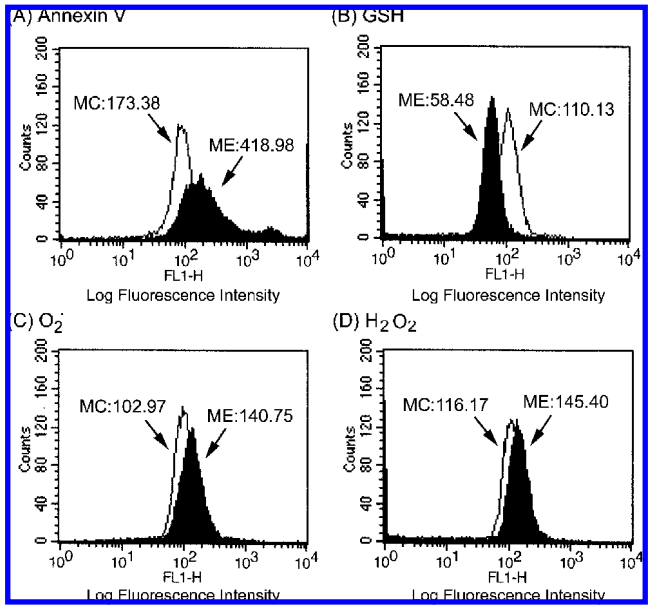

Figure 4. Determination of membrane integrity, cellular content of GSH, and ROS generation in ergocalciferol-treated cells. (**A**) PS translocation in HL-60 cells was monitored by annexin V-FITC staining after 60 μM ergocalciferol treatment for 15 min. (**B**) HL-60 cells were treated with 60 μM ergocalciferol for 30 min and then incubated with fluorescent probe CMFDA for a further 30 min, and the fluorescence in the cells was immediately analyzed by flow cytometry. The generation of (**C**) superoxide anion ($O_2^{\cdot}$) and (**D**) hydrogen peroxide (H_2O_2) within cells was measured by incubation with fluorescent probe DHE or DCHF-DA for 30 min, respectively, after cells were treated with 60 μM ergocalciferol for 60 min. All fluorescence intensities within cells were immediately analyzed using flow cytometry. Data are the average of three independent experiments and represented as log fluorescence intensity. MC, mean of the relative fluorescent emission of control; ME, mean of the relative fluorescent emission of ergocalciferol.

intracellular peroxide were clearly detected, and the means of fluorescence intensity emitted by DHE and DCFH-DA increase from 102.97 to 140.75 (**Figure 4C**) and from 116.17 to 145.40 (**Figure 4D**), respectively. We suggest that, in combination with these findings, loss of GSH by ergocalciferol might accumulate intracellular hydrogen peroxide, altering redox equilibrium and thereby inducing apoptosis.

Involvement of Mitochondrial Dysfunction, Cytochrome *c* Release, and Cleavage of Caspase-9 and -3 in Ergocalciferol-Induced Apoptosis. A decreasing mitochondrial membrane potential ($\Delta\Psi$m) has been shown to be a pivotal factor to control the induction of apoptosis (*40, 41*). Therefore, we investigated the change of $\Delta\Psi$m in ergocalciferol-induced apoptosis. HL-60 cells were treated with 60 μM ergocalciferol for 30 min and then exposed to fluorescent probe DiOC6(3) that is taken up by mitochondria and undergoes a red shift in emission spectrum during changes in $\Delta\Psi$m. **Figure 5A** shows that a reduction in $\Delta\Psi$m was clearly detected at 30 min after exposure of ergocalciferol (the mean of fluorescent intensity was shifted to the left from 94.37 to 120.39%).

Disruption of $\Delta\Psi$m will result in the opening of mitochondrial membrane pores, causing the release of soluble intermembrane proteins, including cytochrome *c*, which contributes to caspase-9 activation and subsequently induces apoptosis. To determine whether the reduction of $\Delta\Psi$m by ergocalciferol could lead to cytochrome *c* release from mitochondria into cytosol, cell lysates were subfractionated and cytosolic cytochrome *c* was determined by Western blotting. Consistent with

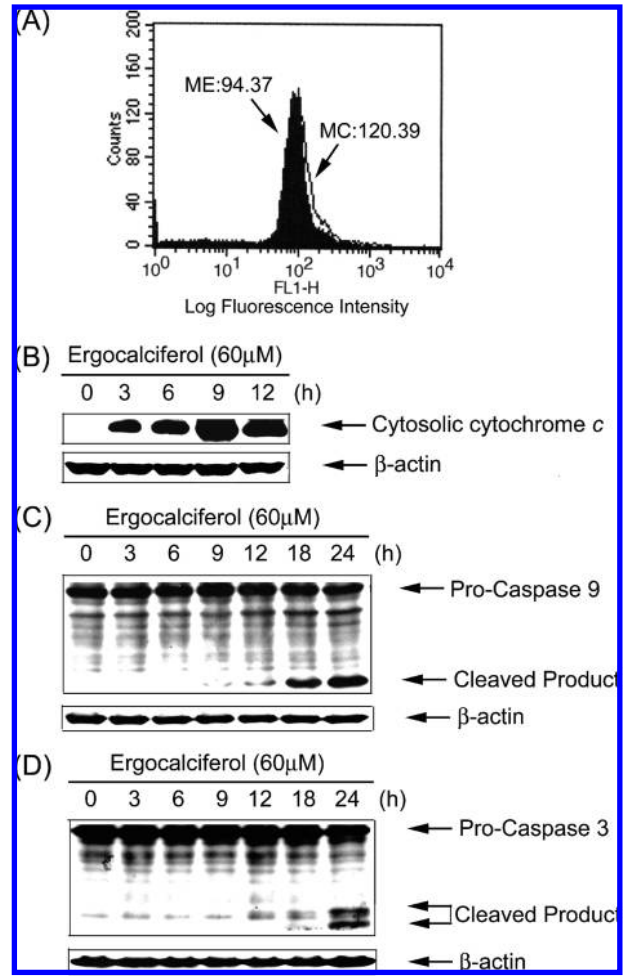

Figure 5. Induction of mitochondria dysfunction and cytochrome *c* release followed by the cleavage of caspase-9 and -3 in ergocalciferol-induced apoptosis. (**A**) HL-60 cells were treated with 60 μM ergocalciferol for 30 min, and the relative $\Delta\Psi$m values were measured by fluorescent emission from DiOC6(3) taken up by mitochondria. The numbers represented the mean of the relative fluorescent intensity. MC, mean of the relative fluorescent emission of control; ME, mean of the relative fluorescent emission of ergocalciferol. (**B**) HL-60 cells were treated with 60 μM ergocalciferol at indicated time periods. Subcellular fractions were prepared as described under Materials and Methods, and cytochrome *c* was detected by Western blotting. (**C**, **D**) Cell lysates of HL-60 after 60 μM ergocalciferol treatment were harvested at the indicated times, and equal amounts of protein (50 μg) from each sample were subjected to Western blotting analysis and probed for caspases-9 and -3. β-Actin served as a loading control.

the timing of loss of $\Delta\Psi$m, cytochrome *c* release into cytosol began at 3 h of exposure of ergocalciferol and increased progressively up to 12 h (**Figure 5B**). To further demonstrate whether cytochrome *c* release by ergocalciferol treatment would subsequently result in the processing of caspase-9, Western blotting was performed to detect the cleavage of pro-caspase-9 by ergocalciferol treatment. Along with the timing of cytochrome *c* release, the time-dependent cleavage of pro-caspase-9 was sequentially observed at 9 h and increased up to 24 h after 60 μM ergocalciferol (**Figure 5C**). These observations suggest that ergocalciferol triggers an apoptosis-inducing mechanism via mitochondria in HL-60 cells.

Because activation of caspase-9 is accompanied by the sequential processing and activation of caspase cascades, for example, caspase-3, the activity of which has been considered

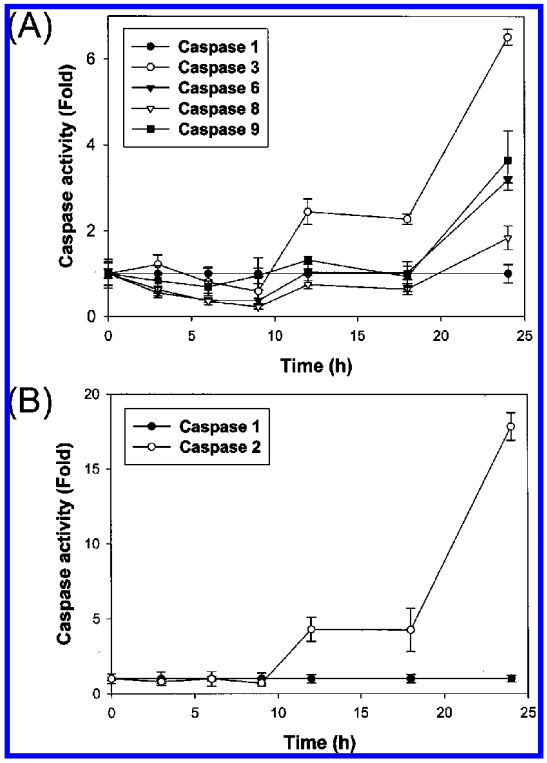

Figure 6. Induction of caspase activities by ergocalciferol in HL-60 cells. (**A**, **B**) Cells were treated with 60 μM ergocalciferol for different times, and the kinetics of caspase activation were assayed as described under Materials and Methods. Data represent means ± SD for three determinations.

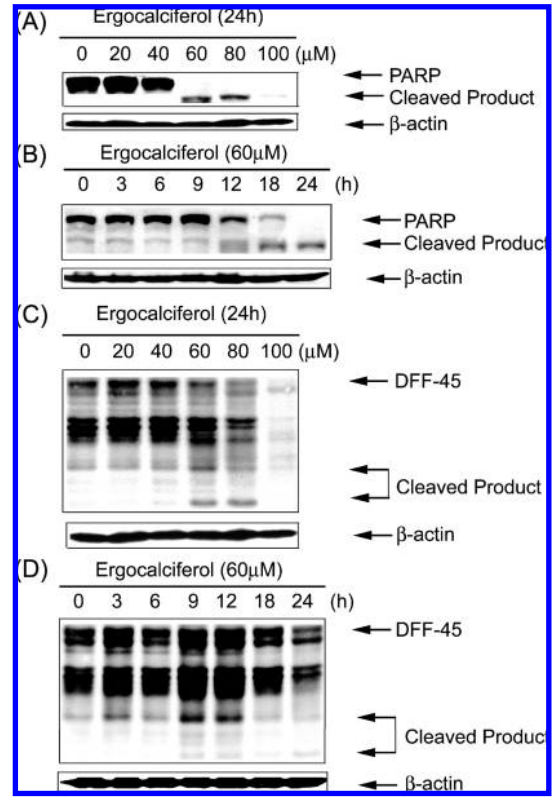

Figure 7. PARP cleavage and DFF-45 degradation by ergocalciferol in HL-60 cells. HL-60 cells were treated with various concentrations of ergocalciferol for 24 h or with 60 μM ergocalciferol for the indicated times, and processing of (**A**, **B**) PARP and (**C**, **D**) DFF-45 was detected by Western blotting analysis using specific antibodies against PARP and DFF-45. β-Actin represented a loading control.

to be essentially involved in many types of stimuli-induced apoptosis (*42, 43*), we next evaluated whether caspase-3 activity would be involved in ergocalciferol-induced apoptosis. **Figure 5D** shows that ergocalciferol led to a time-dependent increase in caspase-3 cleavage, suggesting the activation of caspase cascades in ergocalciferol-induced apoptosis.

Caspase Activation and PARP and DFF-45 Degradation in Ergocalciferol-Treated HL-60 Cells. To determine whether caspases are involved in ergocalciferol-induced apoptosis, we measured the enzymatic activity of caspases using six fluorogenic peptide substrates, Ac-YVAD-AMC, Ac-VDVAD-AMC, Ac-DEVE-AMC, Ac-VEID-AMC, Ac-IETD-AMC, and Ac-LEHD-AMC, which are specific substrates for caspases-1, -2, -3, -6, -8, and -9, respectively. As illustrated in **Figure 6**, showing the kinetic activity of various caspases, ergocalciferol induced a rapid rise in caspase-2, -3, -6, and -9 activities. Notably, the increases in caspase-9 and -3 activities by ergocalciferol are closely correlated with the processing of procaspases-9 and -3, respectively, as demonstrated in **Figure 5C**,**D**. In contrast to the significant increase in caspases-2, -3, -6, and -9, a negligible increase in caspases-1 and -8 was observed.

Caspase-3 activity contributes to the proteolytic cleavage of a number of proteins, such as PARP, which is cleaved by activated caspase-3 to yield the characteristic 85 kDa fragment during apoptosis (*44*). Another caspase-3 substrate is DNA fragmentation factor-45 (DFF-45), which complexes with caspase-activated DNase (CAD), retains CAD in cytosol, and inhibits its function in living cells (*45–47*). During apoptosis, caspase-3 cleaves DFF-45, resulting in the release and activation of CAD, which translocates to nucleus and degrades chromosomal DNA to produce interchromosomal DNA fragmentation. To demonstrate that activation of caspase-3 was followed by the cleavage of PARP and DFF-45 during hop bitter acids-induced apoptosis, the cleavage of PARP and DFF-45 was analyzed by Western blotting as demonstrated in **Figure 7**. The disappearance of 110 kDa PARP was accompanied with the accumulation of the 85 kDa cleaved species after dose treatment of hop bitter acids for 24 h or 60 μM ergocalciferol for 3–24 h, and these observations were dose- and time-dependent (**Figure 7A**,**B**). Similar to PARP cleavage, ergocalciferol also caused a dose- and time-dependent proteolytic cleavage of DFF-45, supporting the findings shown in **Figure 5D**. Taken together, the current data suggest that ergocalciferol would lead to loss of $\Delta\Psi$m and cytochrome *c* release, subsequently activating the caspase cascades, all of which cause the induction of apoptosis in HL-60.

Effects of Ergocalciferol on the Expression of Bcl-2 Family Proteins, Fas, and FasL in HL-60 Cells. Members of the Bcl-2 family of proteins are the most important apoptotic regulators to maintain the integrity of mitochondrial membrane and are located upstream of caspase activation (*48–50*). Members of the Bcl-2 family can be classified as anti- and pro-apoptotic proteins the imbalance of which by certain stimulus is one of the major mechanisms underlying the ultimate fate of cells during apoptosis. To check the change of members of Bcl-2 family during ergocalciferol treatment, the time course effects of ergocalciferol on protein expression of the Bcl-2 family were evaluated by Western blotting. As shown in **Figure 8**, ergocalciferol made the time-dependent induction in pro-apoptotic member Bax but not Bad and Bag-1; however, ergocalciferol promoted anti-apoptotic member Mcl-1 cleavage rather than Bcl-2 and Bcl-X_L. These results suggest that the disordered ratio of Bax and Mcl-1 might play an important role in ergocalciferol-induced apoptosis.

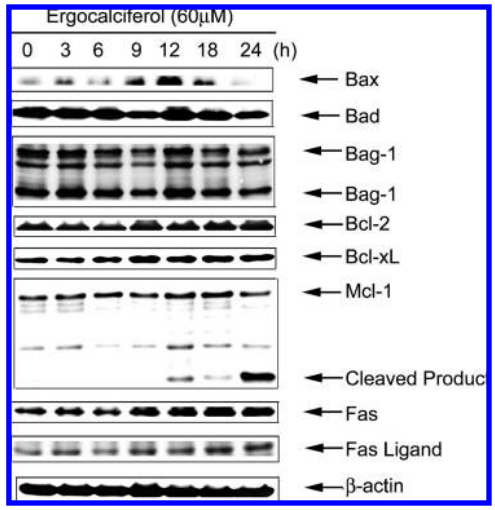

Figure 8. Effects of ergocalciferol on Bcl-2 family protein, Fas, and FasL expression in HL-60 cells. Cells were treated with 60 μM ergocalciferol for times as indicated, and Western blotting analysis was performed to determine the expression of Bcl-2 family proteins, Fas, and FasL. β-Actin represented an internal control for equivalent protein loading.

To assess whether ergocalciferol promoted apoptosis via a receptor-mediated pathway, the levels of Fas and Fas ligand (FasL) proteins were determined by Western blotting. These results exhibit that ergocalciferol stimulated the time-related expression of Fas but not FasL (**Figure 8**, lower panel), allowing us to suggest the possibility that Fas might modulate ergocalciferol-induced apoptosis.

Effects of Antioxidants on Ergocalciferol-Induced Apoptosis in HL-60 Cells. ROS have been known to be important in the induction of apoptosis. We reasoned that ROS scavengers must limit apoptosis. We tested the ROS scavengers catalase (CAT) and *N*-acetylcysteine (NAC) and observed that CAT and NAC markedly protect HL-60 cells from ergocalciferol-induced apoptosis (**Figure 9**). The data from these experiments demonstrate that ROS concentrations influence the result of ergocalcigerol-induced apoptosis and that these concentrations are controlled by the levels of available antioxidants.

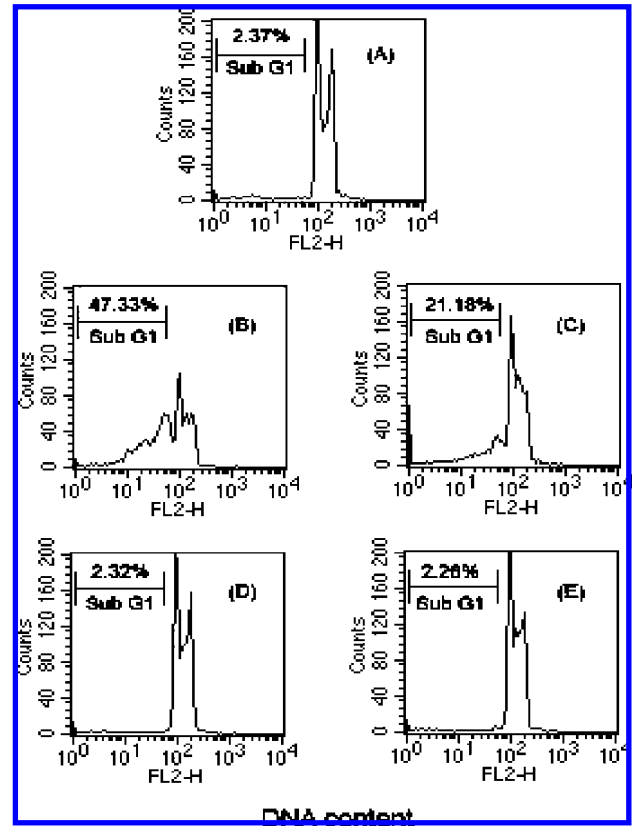

Figure 9. Effect of antioxidants on ergocalciferol-treated HL-60 cells. HL-60 cells were pretreated with catalase and *N*-acetylcysteine for 2 h, followed by treatment with ergocalciferol, and then measured by flow cytometry: (**A**) control; (**B**) 60 μM ergocalciferol; (**C**) ergocalciferol + 400 units/mL CAT; (**D**) ergocalciferol + 2.5 mM NAC; (**E**) ergocalciferol + 5 mM NAC. These experiments were performed at least in triplicate, and a representative experiment is presented.

DISCUSSION

The results in the present study ascertain the capacity of vitamin D_2 to inhibit growth and induce apoptosis in human leukemia cell line HL-60. As shown in **Figures 2**, **3**, and **4A**, vitamin D_2 was the potent and rapid inducer of apoptosis, concurrent with DNA ladder, sub-G1 peak appearance, and PS translocation, respectively. Indeed, treatment with vitamin D_2 caused the activation of caspases-2, -3, -6, and -9, but not caspases-1 and -8, associated with the degradation of PARP and DFF-45, which preceded the onset of apoptosis. Exploring the possible molecular mechanisms underlying HL-60 cell apoptosis by vitamin D_2, we found that the pro-apoptotic activity of vitamin D_2 was accompanied by accumulation of ROS including superoxide anion and hydrogen peroxide (**Figure 4C**,**D**), suggesting that leukemia cell death by vitamin D_2 is a ROS-dependent process. ROS are a family of active molecules containing free radicals and are involved in the modulation of biological cell functions. However, excessive ROS bring about oxidative stresses that cause injury to various cellular constituents such as lipid, protein, and DNA, finally resulting in growth arrest, senescence, or apoptosis (*51, 52*). Intracellular ROS can be generated from aberrant mitochondria, which are well-known as sites of ROS generation and targets for ROS action (*53*). At the early stage of apoptosis, the damaged mitochondria lead to inhibition of oxidation of reducing equivalents in the respiratory chain electron transfer and direct one-electron transfer to O_2 to produce superoxide anion (*54*). Here we demonstrated that vitamin D_2 induced the loss of mitochondrial membrane potential (**Figure 5A**) accompanied with increased ROS generation in HL-60 cells. It provides a possible fundamental explanation for why vitamin D_2 brings about excessive ROS generation in HL-60 cells. We suggest that vitamin D_2 might lead to ROS accumulation by disrupting the integrity of mitochondrial membrane, subsequently interrupting the electron transport assembly and generating ROS by one-electron transfer.

Mitochondria have been suggested as a pivotal mediator in apoptosis triggered by many stimuli (*55*). The function and integrity of mitochondria are based on the modulation of the Bcl-2 family, whose members may be anti-apoptotic or pro-apoptotic, and regulate cell death by controlling the mitochondria membrane permeability during apoptosis (*56*). Herein, we demonstrated that vitamin D_2 could disrupt the function of mitochondria at the early stage of apoptosis and subsequently coordinate caspase activation through the release of cytochrome *c*. We, therefore, inferred that the Bcl-2 family proteins might participate in the event that controlled the change in mitochondrial membrane potential and trigger cytochrome *c* release during vitamin D_2-induced apoptosis. In this study, we found the down-regulation and cleavage of Mcl-1 expression and concomitant up-regulation of Bax expression in vitamin D_2-treated cells (**Figure 8**). The reduced ratio of Mcl-1 to Bax that

correlated inversely with the increase of vitamin D_2 incubation times is consistent with a model wherein the ratio of anti-apoptotic to pro-apoptotic proteins determines cellular susceptibility to apoptosis (*48*).

Besides mitochondrial decay, the other possibility for excessive ROS production by vitamin D_2 in leukemia cells is GSH depletion, as demonstrated in **Figure 4B**. GSH is an important defense mechanism against potentially toxic hydrogen peroxide by glutathione peroxidase, which reduces hydrogen peroxide to water, along with that the oxidation of GSH. Decreased GSH concentrations might be related to susceptibility to injury by vitamin D_2 in leukemia cells. The decrease in GSH levels might be attributable to several different mechanisms. One possibility is that excessive ROS generation modulated by vitamin D_2 facilitates the consumption of GSH. Another possible mechanism is that vitamin D_2 might directly or indirectly diminish GSH synthesis or regeneration. However, the details of how vitamin D_2 caused the decrease in GSH levels are not yet clear and require further study.

A receptor-mediated pathway is another major mechanism for apoptosis. In **Figure 8**, we observed the enhanced expression of Fas, suggesting that at least part of vitamin D_2-induced apoptosis might be due to Fas-mediated death. Fas receptor protein belongs to the TNF receptor superfamily and reacts with its natural ligand (Fas lignad) that elicits apoptosis in sensitive cells (*57*). Following Fas activation by binding to Fas ligand, Fas oligomerizes by itself and recruits specific adaptor proteins, thereby inducing proteolysis and activation of procaspase-8. Caspase-2 has been suggested as another effector relative to Fas signaling. Caspase-2 null lymphoblasts are more susceptible to Fas-mediated death (*58*), and silencing caspase-2 expression by antisense or caspase-2 inhibitor abrogates cytochrome *c* release and subsequent death (*59*). Although neither Fas ligand expression nor caspase-8 activity can be distinctly observed in vitamin D_2-treated HL-60 cells (**Figures 6A** and **8**), vitamin D_2 can activate caspase-2 accompanied with Fas expression (**Figure 6B**). It raises the possibility that Fas death receptor activation is directly linked to the function of caspase-2 by treatment of vitamin D_2 in HL-60 cells. It is yet unclear how vitamin D_2 up-regulated Fas expression in HL-60 cells. One possibility is enhanced vitamin D_2-mediated mitochondrial decay because mitochondrial dysfunction has been suggested to be associated with *Fas* gene expression (*60*), suggesting that vitamin D_2 might damage mitochondria, thereby leading to the overexpression of Fas protein via an undefined pathway. Altogether, the detailed mechanisms of these issues remain to be deciphered.

To evaluate the cancer-preventive benefits of edible mushrooms, we examine the growth-inhibitory efficiency of vitamin D_2, a well-defined bioconstituent of edible mushrooms, on human leukemia HL-60 cells. On the basis of the outcome of this study and the available literature, the mechanisms by which vitamin D_2 causes apoptosis in HL-60 cells are summarized in **Figure 10**. The initial event induced by vitamin D_2 (vit D_2) is likely an induction of ROS, primarily based on the observation that CAT and NAC prevent apoptosis (**Figure 9**) and coordinative modulation of reducing Mcl-1/Bax ratio that facilitates mitochondrial decay (mito decay) with dissipation of $\Delta\Psi m$. Then, cytochrome *c* (cyto *c*) release and excessive ROS production by the damage of mitochondria bring about caspase activation and GSH depletion, leading to final HL-60 cell apoptosis. On the other hand, dysfunction of mitochondria by vitamin D_2 may indirectly up-regulate Fas expression that subsequently activates caspase-2. Active caspase-2 is known as an initiator for caspase signaling and contributes to programmed cell death. The data of this study define the molecular basis of vitamin D_2-mediated apoptosis, which would provide useful information concerning the development of effective cancer prevention agents against leukemia from dietary constituents such as mushrooms or hop.

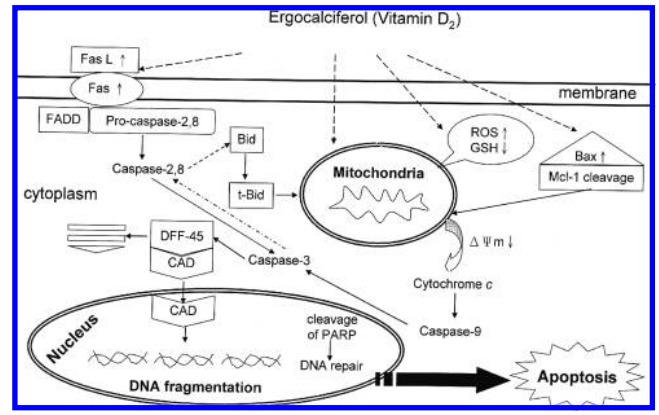

Figure 10. Proposed model of ergocalciferol-mediated human leukemia cell death. See the text for details.

ABBREVIATIONS USED

GSH, glutathione; ROS, reactive oxygen species; PARP, poly (ADP-ribose) polymerase; DFF, DNA fragmentation factor; CAD, caspase-activated DNase; MTT, 3-(4,5-dimethylthiazol-2-yl)-2,5-diphenyltetrazolium bromide; CMFDA, 5-chloromethylfluorescein diacetate; DCHF-DA, dichlorodihydrofluorescein diacetate; DHE, dihydroethidium.

LITERATURE CITED

(1) Agoston, E. S.; Hatcher, M. A.; Kensler, T. W.; Posner, G. H. Vitamin D analogs as anti-carcinogenic agents. *Anticancer Agents Med. Chem.* **2006**, *6* (1), 53–71.

(2) Guyton, K. Z.; Kensler, T. W.; Posner, G. H. Vitamin D and vitamin D analogs as cancer chemopreventive agents. *Nutr. Rev.* **2003**, *61* (7), 227–238.

(3) Magalhaes, P. J.; Carvalho, D. O.; Guido, L. F.; Barros, A. A. Detection and quantification of provitamin D2 and vitamin D2 in hop (*Humulus lupulus* L.) by liquid chromatography-diode array detection-electrospray ionization tandem mass spectrometry. *J. Agric. Food Chem.* **2007**, *55*, 7995–8002.

(4) Bouillon, R.; Eelen, G.; Verlinden, L.; Mathieu, C.; Carmeliet, G.; Verstuyf, A. Vitamin D and cancer. *J. Steroid Biochem. Mol. Biol.* **2006**, *102* (1–5), 156–162.

(5) Jones, G.; Strugnell, S. A.; DeLuca, H. F. Current understanding of the molecular actions of vitamin D. *Physiol. Rev.* **1998**, *78* (4), 1193–1231.

(6) Schwartz, G. G.; Skinner, H. G. Vitamin D status and cancer: new insights. *Curr. Opin. Clin. Nutr. Metab. Care* **2007**, *10* (1), 6–11.

(7) Abe, E.; Miyaura, C.; Sakagami, H.; Takeda, M.; Konno, K.; Yamazaki, T.; Yoshiki, S.; Suda, T. Differentiation of mouse myeloid leukemia cells induced by 1α,25-dihydroxyvitamin D3. *Proc. Natl. Acad. Sci. U.S.A.* **1981**, *78* (8), 4990–4994.

(8) Miyaura, C.; Abe, E.; Kuribayashi, T.; Tanaka, H.; Konno, K.; Nishii, Y.; Suda, T. 1α,25-Dihydroxyvitamin D3 induces differentiation of human myeloid leukemia cells. *Biochem. Biophys. Res. Commun.* **1981**, *102* (3), 937–943.

(9) Chouvet, C.; Vicard, E.; Devonec, M.; Saez, S. 1,25-Dihydroxyvitamin D3 inhibitory effect on the growth of two human breast cancer cell lines (MCF-7, BT-20). *J. Steroid Biochem.* **1986**, *24* (1), 373–376.

(10) Getzenberg, R. H.; Light, B. W.; Lapco, P. E.; Konety, B. R.; Nangia, A. K.; Acierno, J. S.; Dhir, R.; Shurin, Z.; Day, R. S.; Trump, D. L.; Johnson, C. S. Vitamin D inhibition of prostate adenocarcinoma growth and metastasis in the Dunning rat prostate model system. *Urology* **1997**, *50* (6), 999–1006.

(11) Eisman, J. A.; Barkla, D. H.; Tutton, P. J. Suppression of in vivo growth of human cancer solid tumor xenografts by 1,25-dihydroxyvitamin D3. *Cancer Res.* **1987**, *47* (1), 21–25.

(12) Hershberger, P. A.; Modzelewski, R. A.; Shurin, Z. R.; Rueger, R. M.; Trump, D. L.; Johnson, C. S. 1,25-Dihydroxycholecalciferol (1,25-D3) inhibits the growth of squamous cell carcinoma and down-modulates p21(Waf1/Cip1) in vitro and in vivo. *Cancer Res.* **1999**, *59* (11), 2644–2649.

(13) Jones, G.; Byrnes, B.; Palma, F.; Segev, D.; Mazur, Y. Displacement potency of vitamin D2 analogs in competitive protein-binding assays for 25-hydroxyvitamin D3, 24,25-dihydroxyvitamin D3, and 1,25-dihydroxyvitamin D3. *J. Clin. Endocrinol. Metab.* **1980**, *50* (4), 773–775.

(14) Horst, R. L.; Koszewski, N. J.; Reinhardt, T. A. 1α-Hydroxylation of 24-hydroxyvitamin D2 represents a minor physiological pathway for the activation of vitamin D2 in mammals. *Biochemistry* **1990**, *29*, 578–582.

(15) Mawer, E. B.; Jones, G.; Davies, M.; Still, P. E.; Byford, V.; Schroeder, N. J.; Makin, H. L.; Bishop, C. W.; Knutson, J. C. Unique 24-hydroxylated metabolites represent a significant pathway of metabolism of vitamin D2 in humans: 24-hydroxyvitamin D2 and 1,24-dihydroxyvitamin D2 detectable in human serum. *J. Clin. Endocrinol. Metab.* **1998**, *83* (6), 2156–2166.

(16) Jones, G.; Byford, V.; Makin, H. L.; Kremer, R.; Rice, R. H.; deGraffenried, L. A.; Knutson, J. C.; Bishop, C. W. Antiproliferative activity and target cell catabolism of the vitamin D analog 1α,24(S)-(OH)2D2 in normal and immortalized human epidermal cells. *Biochem. Pharmacol.* **1996**, *52* (1), 133–140.

(17) Knutson, J. C.; LeVan, L. W.; Valliere, C. R.; Bishop, C. W. Pharmacokinetics and systemic effect on calcium homeostasis of 1α,24-dihydroxyvitamin D2 in rats. Comparison with 1α,25-dihydroxyvitamin D2, calcitriol, and calcipotriol. *Biochem. Pharmacol.* **1997**, *53* (6), 829–837.

(18) Narvaez, C. J.; Byrne, B. M.; Romu, S.; Valrance, M.; Welsh, J. Induction of apoptosis by 1,25-dihydroxyvitamin D3 in MCF-7 vitamin D3-resistant variant can be sensitized by TPA. *J. Steroid Biochem. Mol. Biol.* **2003**, *84* (2–3), 199–209.

(19) Kumagai, T.; O'Kelly, J.; Said, J. W.; Koeffler, H. P. Vitamin D2 analog 19-nor-1,25-dihydroxyvitamin D2: antitumor activity against leukemia, myeloma, and colon cancer cells. *J. Natl. Cancer Inst.* **2003**, *95* (12), 896–905.

(20) Swamy, N.; Chen, T. C.; Peleg, S.; Dhawan, P.; Christakos, S.; Stewart, L. V.; Weigel, N. L.; Mehta, R. G.; Holick, M. F.; Ray, R. Inhibition of proliferation and induction of apoptosis by 25-hydroxyvitamin D3-3β-(2)-bromoacetate, a nontoxic and vitamin D receptor-alkylating analog of 25-hydroxyvitamin D3 in prostate cancer cells. *Clin. Cancer Res.* **2004**, *10* (23), 8018–8027.

(21) Ashkenazi, A.; Dixit, V. M. Death receptors: signaling and modulation. *Science* **1998**, *281* (5381), 1305–1308.

(22) Green, D. R.; Evan, G. I. A matter of life and death. *Cancer Cell* **2002**, *1* (1), 19–30.

(23) Rao, R. V.; Ellerby, H. M.; Bredesen, D. E. Coupling endoplasmic reticulum stress to the cell death program. *Cell Death Differ.* **2004**, *11* (4), 372–380.

(24) Nakagawa, T.; Zhu, H.; Morishima, N.; Li, E.; Xu, J.; Yankner, B. A.; Yuan, J. Caspase-12 mediates endoplasmic-reticulum-specific apoptosis and cytotoxicity by amyloid-β. *Nature* **2000**, *403* (6765), 98–103.

(25) Kaufman, R. J. Stress signaling from the lumen of the endoplasmic reticulum: coordination of gene transcriptional and translational controls. *Genes Dev.* **1999**, *13* (10), 1211–1233.

(26) Katdare, M.; Jinno, H.; Osborne, M. P.; Telang, N. T. Negative growth regulation of oncogene-transformed human breast epithelial cells by phytochemicals. Role of apoptosis. *Ann. N. Y. Acad. Sci.* **1999**, *889*, 247–252.

(27) Katdare, M.; Osborne, M. P.; Telang, N. T. Inhibition of aberrant proliferation and induction of apoptosis in pre-neoplastic human mammary epithelial cells by natural phytochemicals. *Oncol. Rep.* **1998**, *5* (2), 311–315.

(28) Kim, H. J.; Chang, W. K.; Kim, M. K.; Lee, S. S.; Choi, B. Y. Dietary factors and gastric cancer in Korea: a case-control study. *Int. J. Cancer* **2002**, *97* (4), 531–535.

(29) Poot, M.; Kavanagh, T. J.; Kang, H. C.; Haugland, R. P.; Rabinovitch, P. S. Flow cytometric analysis of cell cycle-dependent changes in cell thiol level by combining a new laser dye with Hoechst 33342. *Cytometry* **1991**, *12* (2), 184–187.

(30) Pan, M. H.; Lin, J. H.; Lin-Shiau, S. Y.; Lin, J. K. Induction of apoptosis by penta-*O*-galloyl-β-D-glucose through activation of caspase-3 in human leukemia HL-60 cells. *Eur. J. Pharmacol.* **1999**, *381* (2–3), 171–183.

(31) Wang, I. K.; Lin-Shiau, S. Y.; Lin, J. K. Induction of apoptosis by lovastatin through activation of caspase-3 and DNase II in leukaemia HL-60 cells. *Pharmacol. Toxicol.* **2000**, *86* (2), 83–91.

(32) Wang, I. K.; Lin-Shiau, S. Y.; Lin, J. K. Induction of apoptosis by apigenin and related flavonoids through cytochrome *c* release and activation of caspase-9 and caspase-3 in leukaemia HL-60 cells. *Eur. J. Cancer* **1999**, *35* (10), 1517–1525.

(33) Pan, M. H.; Chang, W. L.; Lin-Shiau, S. Y.; Ho, C. T.; Lin, J. K. Induction of apoptosis by garcinol and curcumin through cytochrome *c* release and activation of caspases in human leukemia HL-60 cells. *J. Agric. Food Chem.* **2001**, *49* (3), 1464–1474.

(34) Telford, W. G.; King, L. E.; Fraker, P. J. Comparative evaluation of several DNA binding dyes in the detection of apoptosis-associated chromatin degradation by flow cytometry. *Cytometry* **1992**, *13* (2), 137–143.

(35) Fraker, P. J.; King, L. E.; Lill-Elghanian, D.; Telford, W. G. Quantification of apoptotic events in pure and heterogeneous populations of cells using the flow cytometer. *Methods Cell. Biol.* **1995**, *46*, 57–76.

(36) Fernandez-Checa, J. C.; Garcia-Ruiz, C.; Colell, A.; Morales, A.; Mari, M.; Miranda, M.; Ardite, E. Oxidative stress: role of mitochondria and protection by glutathione. *Biofactors* **1998**, *8* (1–2), 7–11.

(37) Paolicchi, A.; Dominici, S.; Pieri, L.; Maellaro, E.; Pompella, A. Glutathione catabolism as a signaling mechanism. *Biochem. Pharmacol.* **2002**, *64* (5–6), 1027–1035.

(38) Simon, H. U.; Haj-Yehia, A.; Levi-Schaffer, F. Role of reactive oxygen species (ROS) in apoptosis induction. *Apoptosis* **2000**, *5* (5), 415–418.

(39) Giles, G. I. The redox regulation of thiol dependent signaling pathways in cancer. *Curr. Pharm. Des.* **2006**, *12* (34), 4427–4443.

(40) Zamzami, N.; Marchetti, P.; Castedo, M.; Decaudin, D.; Macho, A.; Hirsch, T.; Susin, S. A.; Petit, P. X.; Mignotte, B.; Kroemer, G. Sequential reduction of mitochondrial transmembrane potential and generation of reactive oxygen species in early programmed cell death. *J. Exp. Med.* **1995**, *182* (2), 367–377.

(41) Kroemer, G.; Reed, J. C. Mitochondrial control of cell death. *Nat. Med.* **2000**, *6* (5), 513–519.

(42) Nicholson, D. W.; Thornberry, N. A. Caspases: killer proteases. *Trends Biochem. Sci.* **1997**, *22* (8), 299–306.

(43) Salvesen, G. S.; Dixit, V. M. Caspases: intracellular signaling by proteolysis. *Cell* **1997**, *91* (4), 443–446.

(44) Tewari, M.; Quan, L. T.; O'Rourke, K.; Desnoyers, S.; Zeng, Z.; Beidler, D. R.; Poirier, G. G.; Salvesen, G. S.; Dixit, V. M. Yama/CPP32 β, a mammalian homolog of CED-3, is a CrmA-inhibitable protease that cleaves the death substrate poly(ADP-ribose) polymerase. *Cell* **1995**, *81* (5), 801–809.

(45) Liu, X.; Zou, H.; Slaughter, C.; Wang, X. DFF, a heterodimeric protein that functions downstream of caspase-3 to trigger DNA fragmentation during apoptosis. *Cell* **1997**, *89* (2), 175–184.

(46) Sakahira, H.; Enari, M.; Nagata, S. Cleavage of CAD inhibitor in CAD activation and DNA degradation during apoptosis. *Nature* **1998**, *391* (6662), 96–99.

(47) Enari, M.; Sakahira, H.; Yokoyama, H.; Okawa, K.; Iwamatsu, A.; Nagata, S. A caspase-activated DNase that degrades DNA

during apoptosis, and its inhibitor ICAD. *Nature* **1998**, *391* (6662), 43–50.
(48) Oltvai, Z. N.; Milliman, C. L.; Korsmeyer, S. J. Bcl-2 heterodimerizes in vivo with a conserved homolog, Bax, that accelerates programmed cell death. *Cell* **1993**, *74* (4), 609–619.
(49) Tsujimoto, Y. Bcl-2 family of proteins: life-or-death switch in mitochondria. *Biosci. Rep.* **2002**, *22* (1), 47–58.
(50) Tsujimoto, Y. Cell death regulation by the Bcl-2 protein family in the mitochondria. *J. Cell. Physiol.* **2003**, *195* (2), 158–167.
(51) Finkel, T.; Holbrook, N. J. Oxidants, oxidative stress and the biology of ageing. *Nature* **2000**, *408* (6809), 239–247.
(52) Martindale, J. L.; Holbrook, N. J. Cellular response to oxidative stress: signaling for suicide and survival. *J. Cell Physiol.* **2002**, *192* (1), 1–15.
(53) Skulachev, V. P. Mitochondrial physiology and pathology; concepts of programmed death of organelles, cells and organisms. *Mol. Aspects Med.* **1999**, *20* (3), 139–184.
(54) Turrens, J. F. Superoxide production by the mitochondrial respiratory chain. *Biosci. Rep.* **1997**, *17* (1), 3–8.
(55) Green, D. R.; Reed, J. C. Mitochondria and apoptosis. *Science* **1998**, *281* (5381), 1309–1312.
(56) Adams, J. M.; Cory, S. The Bcl-2 protein family: arbiters of cell survival. *Science* **1998**, *281* (5381), 1322–136.
(57) Suda, T.; Takahashi, T.; Golstein, P.; Nagata, S. Molecular cloning and expression of the Fas ligand, a novel member of the tumor necrosis factor family. *Cell* **1993**, *75* (6), 1169–1178.
(58) Bergeron, L.; Perez, G. I.; Macdonald, G.; Shi, L.; Sun, Y.; Jurisicova, A.; Varmuza, S.; Latham, K. E.; Flaws, J. A.; Salter, J. C.; Hara, H.; Moskowitz, M. A.; Li, E.; Greenberg, A.; Tilly, J. L.; Yuan, J. Defects in regulation of apoptosis in caspase-2-deficient mice. *Genes Dev.* **1998**, *12* (9), 1304–14.
(59) Droin, N.; Bichat, F.; Rebe, C.; Wotawa, A.; Sordet, O.; Hammann, A.; Bertrand, R.; Solary, E. Involvement of caspase-2 long isoform in Fas-mediated cell death of human leukemic cells. *Blood* **2001**, *97* (6), 1835–1844.
(60) Asoh, S.; Mori, T.; Hayashi, J.; Ohta, S. Expression of the apoptosis-mediator Fas is enhanced by dysfunctional mitochondria. *J. Biochem. (Tokyo)* **1996**, *120* (3), 600–607.

Received for review October 18, 2007. Revised manuscript received February 15, 2008. Accepted February 20, 2008. This study was supported by the National Science Council under Grants NSC 96-2321-B-022-001, NSC 95-2313-B-022-003-MY3, NSC 95-2320-B-040-037, and NSC 96-2320-B-040-023.

JF0730744